Quantum dynamics simulations of photodissociation reactions

ARTICLE *in* INTERNATIONAL JOURNAL OF QUANTUM CHEMISTRY · MARCH 2006

Impact Factor: 1.43 · DOI: 10.1002/qua.20829

4 AUTHORS, INCLUDING:

Marie-Christine Bacchus-Montabonel
Claude Bernard University Lyon 1
115 PUBLICATIONS **904** CITATIONS
SEE PROFILE

Nathalie Vaeck
Université Libre de Bruxelles
93 PUBLICATIONS **997** CITATIONS
SEE PROFILE

Michèle Desouter-Lecomte
Université Paris-Sud 11
80 PUBLICATIONS **1,082** CITATIONS
SEE PROFILE

Quantum Dynamics Simulations of Photodissociation Reactions

B. LASORNE,[1] M. C. BACCHUS-MONTABONEL,[2] N. VAECK,[3] M. DESOUTER-LECOMTE[2,4]

[1]*Laboratoire de Chimie Physique, CNRS et Université Paris-Sud, 91405 Orsay Cedex, France*

[2]*Laboratoire de Spectrométrie Ionique et Moléculaire, CNRS et Université Lyon I, 43 Bd. du 11 Novembre 1918, 69622 Villeurbane Cedex, France*

[3]*Laboratoire de Chimie Quantique et Photophysique, CP 160/09 Université Libre de Bruxelles, 50 Av. F. Roosevelt, B-1050 Bruxelles, Belgium*

[4]*Département de Chimie, Université de Liège, Sart-Tilman B6, Liège 4000, Belgium*

Received 20 June 2004; accepted 13 October 2004
Published online 17 October 2005 in Wiley InterScience (www.interscience.wiley.com).
DOI 10.1002/qua.20829

ABSTRACT: Wave packet simulations using ab initio potential energy surfaces (PES) have been developed within the framework of the constrained Hamiltonian methodology. The approach is presented with the example of bromoacetyl chloride photodissociation. Int J Quantum Chem 106: 670–675, 2006

Key words: wave packet simulations; quantum dynamics; photodissociation reactions; ab initio potential energy surfaces

Introduction

Quantum molecular dynamics modeling the time evolution of a chemical system by directly solving the Schrödinger equations has been proved efficient in a number of cases. Nevertheless, for large polyatomic molecules (more than four/five atoms), a full quantum treatment is prohibitive, and it is necessary to make use of dimensionality reduction techniques. The MCTDH method [1] appears to be a very promising multidimensional quantum approach. However, a number of chemical events involve few nuclear degrees of freedom to change the molecular frame. In some systems of biological interest, this could even be a way for a process to keep its efficiency by avoiding dissipation of the energy [2]. In that sense, the wave packet time-dependent methods offer the possibility of separating the total configuration space into a subspace of n internal active coordinates q, which are quantum mechanically treated on ab initio potential energy surfaces (PES), while the inactive coordinates Q are implicitly taken into account. We adopt the constrained Hamiltonian methodology to account for the spectator coordinates considered as classical functions of the active ones $Q(q)$ [3, 4]. The

Correspondence to: M. C. Bacchus-Montabonel; e-mail: bacchus@lasim.univ-lyon1.fr

potential energy surfaces (PES) are determined by ab initio calculations. The corresponding kinetic energy operators are numerically but exactly computed by means of the T_{num} algorithm [5].

This approach is presented with the example of the competitive photodissociation of bromoacetyl chloride upon [$n_O \rightarrow \pi^*_{CO}$] excitation by photolysis at 248 nm [6]. By measuring the photofragment velocities and angular distributions in crossed laser molecular beam experiments, with ^{79}Br and ^{35}Cl isotopes, the experimental C—Cl:C—Br branching ratio is ~1.0:0.4, while only a minor contribution may be attributed to the C—C fission channel [7, 8]. Paradoxically, the stronger C—Cl bond cleavage dominates over the fission of the weaker C—Br bond. For unimolecular dissociation in a single electronic state, statistical theories predict that a weaker bond breaks preferentially over a stronger one according to the barrier heights at the transition states. By ab initio structure calculations performed for the *trans* (Cl and Br) and C_s conformer using a STO-3G* basis set at the CIS and CISD computational level, the difference of the energy barriers was first estimated to ~10 kcal · mol^{-1} [7]. Butler and coworkers [7, 8] then argued that a nonadiabatic interaction between the first two $^1A''$ excited electronic states could qualitatively explain the inverted branching ratio. The top of the barrier corresponds here to an avoided crossing between the [$n_O \rightarrow \pi^*_{CO}$] and [$n_X \rightarrow \sigma^*_{CX}$] (X = Br or Cl) excited states. If the splitting is very small, one can observe a trapping in the diabatic potential surface leading to a very small dissociation probability. Such a recrossing of the transition state strongly decreases the pre-exponential factor of the statistical theory and could explain the experimental branching ratio. This interesting problem has also been analyzed by a phase space statistical model, using Butler's data [9]. Recently, this mechanism based on nonadiabatic interactions was criticized by Ding et al. [10]. From CASSCF(8,7) calculations of the stationary equilibrium and transition structures, the authors conclude that the results reported by Butler's group overestimate the barrier heights and underestimate the energy splitting between the first two $^1A''$ excited states. They propose that the main factor explaining the selectivity of the C—Cl and C—Br bond cleavage is a distance dependence of intramolecular energy redistribution. Unfortunately, this work does not give any estimation of the energy gaps or nonadiabatic couplings.

To gain a more precise insight into this mechanism, in particular to evaluate the importance of nonadiabatic effects, we have revisited this problem and performed a dynamical treatment by means of a time-dependent wave packet approach [11, 12]. We present here an overview of the different steps of our investigation, with probe of the initial relaxation in the first excited electronic state by propagating two-dimensional (2D) wave packets in the subspace of the C═O bond and the torsion angle breaking the C_s symmetry. This determines the relevant geometry for a one-dimensional (1D) model of the nonadiabatic dissociation along the C—Cl or C—Br stretching. We then investigate more deeply the process by checking the role of the variation of the C═O bond length in 2D wave packet simulations on CO/CCl and CO/CBr subspaces.

Theoretical Framework

CONSTRAINED HAMILTONIAN METHODOLOGY

The general form of the constrained vibrational Hamiltonian associated with a single electronic state and zero total angular momentum is

$$\hat{H}_{n-D} = \hat{T}_q + V[q, Q(q)] = \sum_{i,j=1}^{n} f_2^{ij}(q)\partial^2_{q_i q_j} + f_1^{ij}(q)\partial_{q_j} + \nu(q) + V[q, Q(q)],$$

where $V[q, Q(q)]$ is the projection of the whole PES $V(q, Q)$ and $v(q)$, the extrapotential term due to the choice of the normalization convention. The inactive coordinates Q are implicitly taken into account in the expression of the kinetic functions f_2^{ij} (**q**), f_1^{ij} (q), and $v(q)$, either in the rigid-constraint approach, which consists of freezing some bond lengths, angles, or entire atomic groups, or in the adiabatic-constraint approach by adjusting the variation of the inactive coordinates to those of the few active ones by means of local potential minimizations. In this work, we have used rigid models by computing cuts $V(q, Q_0)$ for various geometries Q_0. The precise values of the kinetic functions are generated numerically by the T_{num} algorithm [5], using the Z-matrix coordinates, which facilitate description of large-amplitude movements of given atoms.

Such an approach is particularly suitable for checking the role of different active subspaces and different hypothesis on the inactive skeleton. 1D wave packet simulations of the C—Cl and C—Br dissociation have been performed on the adiabatic

coupled states using the Chebyshev scheme [13]. In the case of the 2D dynamics on CO/CCl and CO/CBr surfaces, we have introduced a diabatic model in order to adopt the less consuming split operator technique [14] and used orthogonalized pseudo-Cartesian coordinates to solve the time-dependent close coupling equations with an approximate kinetic energy operator built from the T_{num} kinetic grids.

AB INITIO CALCULATIONS

The ab initio study of this large molecular system is particularly challenging since it concerns excited states. Molecular calculations were carried out using the MOLPRO suite of ab initio programs [15]. Correlation-consistent VDZ basis sets of Dunning [16] were used for all atoms. Tests have been performed with the more diffuse 6-311G** basis set and they demonstrate that the choice of the VDZ basis set is quite sufficient in this study. The molecular orbitals were optimized in state average CASSCF calculations of the two $^1A''$ excited states involved in the photodissociation process in the C_s symmetry group. The active space includes all the valence orbitals augmented of the π^*_{CO} (a'' symmetry), σ^*_{CCl}, σ^*_{CBr} (a' symmetry) orbitals.

MRCI calculations of the transition energy have been performed. At the MRCI level of theory, the transition energy is 100.5 kcal $\cdot$ mol^{-1}, clearly showing good accuracy for our CASSCF calculation, which provides nearly the same transition energy value (100.6 kcal $\cdot$ mol^{-1}). These results compare reasonably with the calculations of Ding et al. [10].

Results

ACTIVE MODES

In such a problem, a deep interaction between dynamics and ab initio calculations is necessary to choose the relevant active subspaces. First, a hierarchy among the intramolecular degrees of freedom has to be established by comparing their typical time scale with the C—Cl and C—Br dissociation time and by analyzing the different kinetic-energy-operator terms. Spin-orbit coupling has not been considered in this work.

An optimization of the geometry in the ground and excited state with *trans* constraints shows, in particular, a strong elongation of the C═O chemical bond [11] in the excited state that can be directly related to the [$n_O \rightarrow \pi^*_{CO}$] first excitation in the Franck–Condon region. The C═O coordinate appears thus to be essential to describe the photodissociation process. In contrast, completely different behaviors are observed for the ground and excited potential energy curves toward the torsion mode ϕ = Br—C—C—Cl. Indeed, the minimum energy of the ground state is obtained in the *trans* conformation with two local minima for the *gauche* conformers around a torsion angle of 61°, when the first excited state presents two clear symmetrical minima for the *gauche* conformer at ~90°. It is therefore natural to expect motion along the internal coordinate ϕ to play an important role in the initial relaxation step of the photodissociation mechanism.

Initial Relaxation

After Franck–Condon excitation, the electronic state is at the top of the torsion excited barrier in the *trans* conformation, with a short C═O bond distance. Therefore, as supported by consideration of ground state vibrational frequencies [17], a redistribution of the excitation energy along these two coordinates in a time scale shorter than the molecular dissociation can be expected. We have calculated the PES as a function of the C═O bond length and the torsion angle for the lowest excited state, the inactive coordinates being frozen either in the Franck–Condon geometry (sudden approximation) or in the excited *trans* geometry (very fast relaxation of all the other modes). At each of these geometries, the energy difference between the two first $^1A''$ states is large and no nonadiabatic effect is expected. Gaussian initial wave packets have been prepared in the Franck–Condon region with widths estimated from the ground state force constants [17]. Their propagation on 2D surfaces shows that the C═O elongation movement is faster than the torsion that appears to be too slow to play a determinant role in the relaxation process, in both relaxed and Franck–Condon geometries. The torsional motion can thus be removed from the active coordinates and the dissociation dynamics will be treated in the *trans* geometry. Moreover, the average expectation value of the C═O length obtained in the wave packet simulation corresponds roughly to the value R_{CO} = 0.1347 nm observed in the excited state. The system is thus expected to exhibit a very fast relaxation and all the inactive coordinates have been frozen at their equilibrium value in the excited *trans* and C_s conformer.

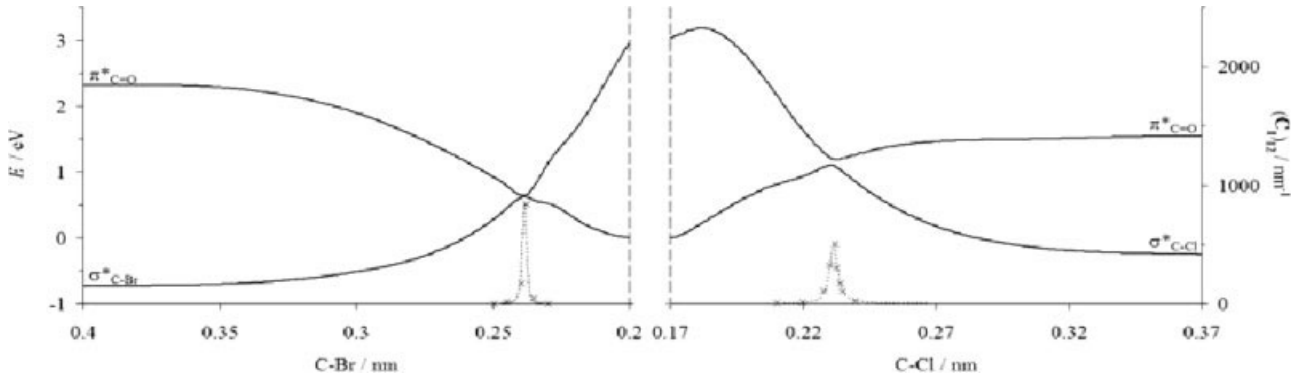

FIGURE 1. Excited $^1A''$ adiabatic potential energy curves and couplings in the *trans* geometry. Energy is measured in eV above the excited *trans* TS.

The O—C—C—Cl variation related to the wagging pyramidalization due to the C═O bond excitation has been discarded in this study. It is certainly justified for the dissociation of C—Br, as suggested by the transition state structure calculated by Ding et al. [10]. In the C—Cl case, we make the assumption that the wagging deformation time scale is smaller than the molecular lifetime. This is supported by a comparative analysis of the cross-term coefficients obtained by T_{num}, which show clearly that the intramolecular energy exchange among the CO stretching and both torsion and wagging is not favored. A similar behavior for the CO/wagging and CO/torsion subspaces can thus be expected.

DISSOCIATION PROCESS

1D Nonadiabatic Dissociations

We have taken account separately of the two dissociation channels after relaxation of all the other coordinates in the excited *trans* geometry. The potential energy curves and couplings for elongation of the C—Cl and C—Br bonds in the excited $^1A''$ states are presented in Figure 1. They show a very sharp avoided crossing between the excited $[n_O \rightarrow \pi^*_{CO}]$ level and the $^1A''$ state leading to the homolytic breaking $[n_X \rightarrow \sigma^*_{CX}]$. The energy barrier is 7.5 kcal · mol^{-1} lower for the breaking of the C—Br bond than for the C—Cl dissociation. Normally, the C—Br dissociation channel would be favored. On the contrary, the C—Cl stretching exhibits a larger energy difference between the two $^1A''$ states, as well as a less sharp radial coupling matrix element leading to the preferential adiabatic dissociation of the C—Cl bond, while C—Br movement is expected to behave diabatically.

As proposed in previous work [18], Gaussian wave packets have been prepared in the Franck–Condon region with ground state widths [17] for the same mean available energy for the two dissociations, in the range 1.5–2.7 eV above the minimum of the excited state. The branching ratio estimated from the asymptotic populations C—Cl:C—Br varies from 1.0:0.17 for 2.7 eV to 1.0:0.24 for 1.5 eV, of the same order of magnitude, but smaller, than the experimental result of C—Cl:C—Br = 1.0:0.4. The theoretical result remains stable when varying the ratio of the energy distributed between the two modes.

This simulation reproduces a preferential breaking along the C—Cl chemical bond with a smooth variation with the energy. The dissociation probability slightly increases with energy for C—Cl but decreases for C—Br, which explains the behavior of the branching ratio with energy. But clearly both dissociation modes depend on the CO bond length variation, and we have thus performed 2D simulations in the two CO/CX (X = Br, Cl) subspaces to emphasize the role of the C═O vibration upon the $[n_O \rightarrow \pi^*_{CO}]$ excitation.

2D Simulations on the CO/Cl and CO/CBr Subspaces

In that case, wave packet simulations on adiabatic PES would be prohibitive. The adiabatic states are strongly coupled in each CO/CX subspace along a line of quasi-degeneracy leading to sharp peaked coupling matrix elements. Zero-order diabatic PES can thus be derived and are pretty well

TABLE I
Optimized diabatic model parameters.

	CO/CBr	CO/CCl
C	16.7	6.84
E_0	−0.061	−0.003
β	2.39	2.18
D	0.100	0.092
α	1.84	2.65
x_{eq}	2.03	1.69
D_1	0.123	0.200
β_1	2.20	2.30
y_{eq1}	1.389	1.312
D_2	0.277	0.267
β_2	2.29	2.84
y_{eq2}	1.213	1.257
w	0.00077	0.00170

* Energy in hartree and length in Ångstroms.

described by very simple analytical expressions formed by two Morse potentials along the x = d_{CX} and y = d_{CO} coordinates, respectively.

$$V_{11}(x, y) = D_1[1 - e^{-\alpha_1(y-y_{eq1})}]^2 + D[1 - e^{-\alpha(x-x_{eq})}]^2,$$

$$V_{22}(x, y) = D_2[1 - e^{-\alpha_2(y-y_{eq2})}]^2 + Ce^{-\beta x} + E_0.$$

The zero energy is put at the minimum of $V_{11}(x,y)$, which corresponds mainly to the $[n_O, \pi^*_{CO}]$ configuration. $V_{22}(x,y)$ is associated with the $[n_X, \sigma^*_{CX}]$ configuration. Since the states become quasi-degenerate at the crossing point, the determination of the potential coupling V_{12} from the adiabatic energy gap is not very accurate. Consequently, in a first approximation, V_{12} is put as a constant $V_{12} = w$ and considered as a parameter of the model. Finally, all the parameters of V_{11}, V_{22} and w are optimized in order to recover ab initio adiabatic energies with the best accuracy. The optimized parameters are gathered in Table I. The accuracy measured by the mean quadratic deviation, is 4.6 10^{-5} a.u. in the CO/CBr case with w = 0.00077 a.u., and 1.4 10^{-3} a.u. in the CO/CCl one with w = 0.00170 a.u. The nonadiabatic coupling matrix elements corresponding to this diabatic model compare favorably to the ab initio calculations. They are close to Lorentzian functions and nearly isotropic, numerically.

Coupled equations have been solved by the split operator scheme, using the orthogonalized coordinates and constrained Hamiltonian for each diabatic state. As the initial step evidenced experimentally is an excitation to the first excited state $[n_O \rightarrow \pi^*_{CO}]$, the initial wave packets have been taken as products of Gaussian functions put in this lower excited state, nonadiabatic couplings induce possible jump of the wave packets to the dissociation channels $[n_X \rightarrow \sigma^*_{CX}]$. Since the model gives no information about the way the excess energy (due to the excess energy of the photon and to the partial relaxation) is shared out between CO and CX, we make the assumption that every wave packet has an initial impulse in the dissociative mode only. This choice can be considered as artificial, but C—Br and C—Cl dissociations are compared under similar conditions.

The Franck–Condon wave packet is prepared in the neighborhood of the seam in each CO/CX subspace. The first movement is principally the C═O elongation, which drives the wave packet in a motion nearly parallel to the seam in both subspaces and does not lead to any transition. It is only during the second half-oscillation that the packet cuts the seam. Therefore, very strong nonadiabatic transitions occur that give rise to a diabatic trapping in the $[n_O \rightarrow \pi^*_{CO}]$ excited state and only a small population transfer toward the dissociative diabatic state. The time-dependent population on the dissociative diabatic state is presented in Figure 2, as well as the C═O bond length and compared with the previous 1D simulation. The nonadiabatic transition is delayed with regard to the previous 1D simulation by ~20–30 fs due to the dominant C═O motion. The population transfer is slightly larger in the CO/CCl subspace in agreement with experiment, and it is possible to reproduce the experimental C—Cl:C—Br branching ratio 1.0:0.4.

Concluding Remarks

Using wave packet simulations, we have shown that the preferential breaking of the C—Cl bond versus the weaker C—Br bond can be explained by nonadiabatic interactions at avoided crossings, leading to a stronger trapping of the C—Br population. Obviously, this does not prove that it is the correct mechanism, and the results are not quantitative and prospective. However, the branching ratio obtained by propagating Franck–Condon wave packets in the two CO/CCl and CO/CBr subspaces is very satisfactory and allows us to consider this mechanism. The CO elongation cannot be discarded and plays an important role in determining

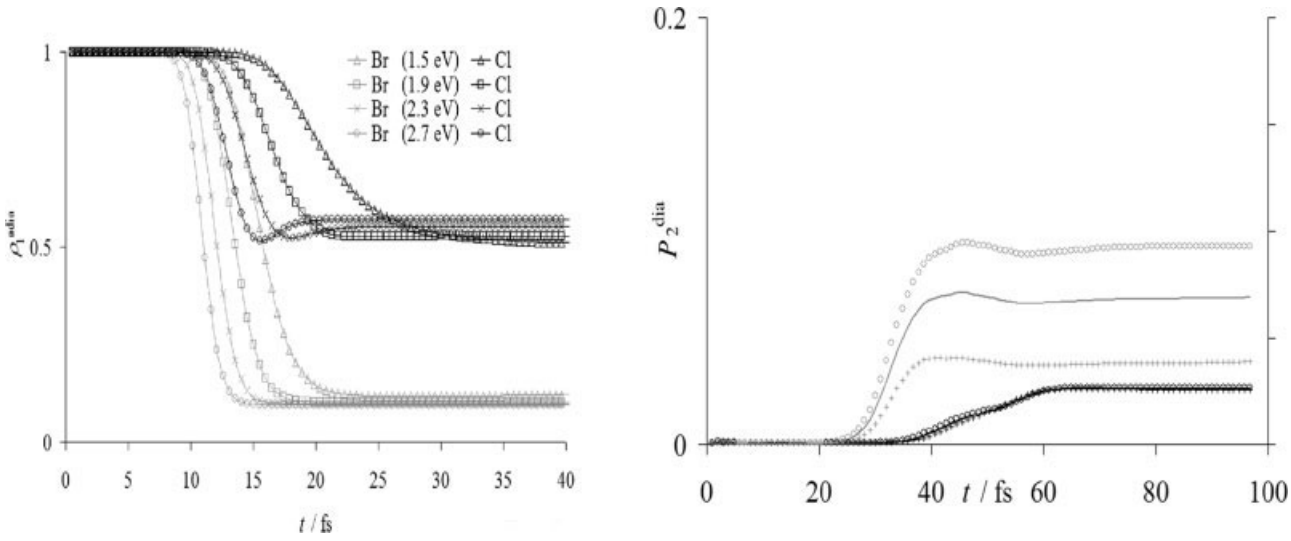

FIGURE 2. Comparison of the time dependent probabilities in the 1D and 2D simulations. Left-hand side: 1D simulations on adiabatic PES, adiabatic population on the first excited state. Right-hand side: 2D simulations on the CO/CCl and CO/CBr diabatic surfaces, probability to jump to the dissociative excited state. Black, CO/CBr; gray, CO/CCl. Open circles, $\langle \hat{H} \rangle = 2.12$ eV, branching ratio 1.0:0.3; full lines, $\langle \hat{H} \rangle = 2.04$ eV, branching ratio 1.0:0.4; plus signs, $\langle \hat{H} \rangle = 1.96$ eV, branching ratio 1.0:0.7.

the way in which the seam is probed by wave packets.

In such an investigation, the choice of the relevant active subspaces is determinant, and a deep interaction between dynamics and ab initio computation is essential. A preliminary analysis of wave packet behavior helps determine what modes can be frozen during a fast dissociation. This strategy has been used to assess that the competitive dissociation can be treated in the *trans* and C_s constrained geometry, by neglecting the internal torsion and wagging in the CO/CCl subspace, in a first approach.

ACKNOWLEDGMENTS

The computing facilities of IDRIS Project 31566 are gratefully acknowledged.

References

1. Beck, M. H.; Jäckle, A.; Worth, G. A.; Meyer, H. D. Phys Rep 2000, 1, 324.
2. Zewail, A. H. J Phys Chem A 2000,104, 5660.
3. (a) Menou, M.; Chapuisat, X. J Mol Spectrosc 1993, 159, 300. (b) Gatti, F.; Justum, Y.; Menou, M.; Nauts, A.; Chapuisat, X. J Mol Spectrosc 1997, 181, 403.
4. Hadder, J. B.; Frederick, J. H. J Chem Phys 1992, 97, 3500.
5. Lauvergnat, D.; Nauts, A. J Chem Phys 2002, 116, 8560.
6. Nakamura, H. Nonadiabatic Transitions: Concepts, Basic Theories and Applications; World Scientific: Singapore, 2002; p 13.
7. Person, M. D.; Kash, P. W.; Butler, L. J. J Chem Phys 1992, 97, 355.
8. Kash, P. W.; Waschewsky, G. C. G.; Butler, L. J.; Francl, M. M. J Chem Phys 1993, 99, 4479.
9. Marks, A. J. J Chem Phys 2001, 114, 1700.
10. Ding, W. J.; Fang, W. H.; Liu, R. Z.; Fang, D. C. J Chem Phys 2002, 117, 8745.
11. Bacchus-Montabonel, M. C.; Vaeck, N.; Lasorne, B.; Desouter-Lecomte, M. Chem Phys Lett 2003, 374, 307.
12. Lasorne, B.; Bacchus-Montabonel, M. C.; Vaeck, N.; Desouter-Lecomte, M. J Chem Phys 2004, 120, 1271.
13. Vaeck, N.; Bacchus-Montabonel, M.-C.; Baloïtcha, E.; Desouter-Lecomte, M. Phys Rev A 2001, 63, 042704.
14. (a) Feit, M. D.; Fleck, J. A., Jr.; Steiger, A. J Comput Phys 1982, 47, 412; (b) Feit, M. D.; Fleck, A. J., Jr. J Chem Phys 1983, 78, 301.
15. Werner, H. J.; Knowles, P., with Almlöf, J.; Amos, R. D.; Berning, A.; Cooper, D. L.; O'Deegan, M. J.; Dobbyn, A. J.; Eckert, F.; Elbert, S. T.; Hampel, C.; Lindh, R.; Lloyd, A.; Meyer, W.; Nicklass, A.; Peterson, K.; Pitzer, R.; Stone, A. J.; Taylor, P. R.; Mura, M. E.; Pulay, P.; Schütz, M.; Stoll, H.; Thorsteinsson, T. MOLPRO; version 2000.1.
16. (a) Dunning, T. H. J Chem Phys 1989, 90, 1007; (b) Woon, D. E.; Dunning, T. H. J Chem Phys 1994, 100, 2975.
17. Durig, J. R.; Shen, Q.; Hagen, K. J Mol Struct 1980, 66, 181.
18. Yokoyama, K.; Yokoyama, A. J Chem Phys 2001, 114, 1624.